High-order unraveling of master equations for dissipative evolution

J. Steinbach,* B.M. Garraway, and P.L. Knight
Optics Section, The Blackett Laboratory, Imperial College, Prince Consort Road, London, SW7 2BZ, United Kingdom
(Received 21 September 1994)

We show how the quantum trajectory method for describing the dissipative evolution of conditioned states can be implemented in a numerically efficient higher-order unraveling that goes beyond the Euler method usually employed in such simulations. We demonstrate its applicability through an analysis of spontaneous emission and find that improvements by two orders of magnitude are possible for the specific example addressed.

PACS number(s): 42.50.Lc

I. INTRODUCTION

The traditional way of treating dissipative coupling between a source system and a large reservoir employs a linear Liouville equation for the system reduced density operator [1]. This describes the evolution of the system reduced density operator ρ_S, having traced out the states of the reservoir, through the irreversible master equation

$$\frac{d}{dt}\rho_S = \mathcal{L}\rho_S\,, \tag{1}$$

where the Liouvillian $\mathcal{L}$ can be decomposed into two parts: a coherent part $\mathcal{L}_0$, which describes the (reversible) coherent dynamics driven by the system Hamiltonian H_S, and a dissipative part $\mathcal{L}_1+\mathcal{L}_2$, describing the system damping through its coupling to the reservoir. We write

$$\begin{aligned}\mathcal{L}\rho_S &= \mathcal{L}_0\rho_S + \mathcal{L}_1\rho_S + \mathcal{L}_2\rho_S \\ &= \frac{i}{\hbar}[\rho_S, H_S] - \frac{1}{2}\left(C^\dagger C\rho_S + \rho_S C^\dagger C\right) + C\rho_S C^\dagger\,. \end{aligned}\tag{2}$$

The Lindblad operator C [2] acts on the small system and as written here represents the coupling to a zero temperature reservoir. In spontaneous emission from an excited atom, for example, the relevant Lindblad operator $C \propto \sigma^-$, the atomic lowering operator, whereas for cavity field-mode damping, the Lindblad operator $C \propto a$, the annihilation operator. Simulation or Monte Carlo methods to describe the evolution of single realizations of systems described by the relevant master equations have been developed [3–5] based on continuous measurement theory [6,7]. Photoelectric detection monitors quanta that irreversibly decay into the reservoir which provides conditioning information that interrupts the coherence of the system dynamics [8]. One method which has received a great deal of attention recently is the Monte Carlo method that simulates the evolution of trajectories in Hilbert space [4,5,9–12] conditioned on continuous photodetection with two distinct elements. The first is smooth evolution under the influence of a non-Hermitian Hamiltonian $H_{\rm eff}$ [Eq. (3)] which originates from the first and second term ($\mathcal{L}_0$ and $\mathcal{L}_1$) in Eq. (2); the second element consists of a stochastic influence that randomly interrupts the non-Hermitian evolution by projections [Eq. (4)] or quantum jumps, determined by the last term in Eq. (2) ($\mathcal{L}_2$):

$$|\Psi\rangle \longrightarrow \exp\left(-\frac{i}{\hbar}H_{\rm eff}\,\delta t\right)|\Psi\rangle\,, \tag{3}$$

$$|\Psi\rangle \longrightarrow C|\Psi\rangle\,, \tag{4}$$

where

$$H_{\rm eff} = H_S - \frac{i\hbar}{2}C^\dagger C\,. \tag{5}$$

Apart from providing insight (especially into the behavior of single realizations [13,14]) into dissipative coupling to a reservoir, any method that evolves a state vector rather than a density matrix requires less memory on a computer than a numerical integration of the master equation. This can make otherwise difficult problems treatable. On the other hand, the sampling process involved in the Monte Carlo method requires the integration of the state vector to be repeated many times before an average is obtained to describe an ensemble of dissipative systems, and associated moments. The procedure has been implemented in two ways. One of them involves making use of a delay function in which the waiting time distribution for photon detection needs to be calculated [3]. A second approach involves discretizing time into finite steps δt [4] and at every step deciding whether or not a quantum jump occurs. The latter is essentially based on a first-order unraveling of the master equation, which makes it disadvantageous when compared with a direct integration, which one might think of implementing with a more accurate and stable higher-order Runge-Kutta method. We follow the suggestion given in [5] and perform the non-Hermitian evolution [Eq. (3)] with a fourth-order integration technique. However, this does not remove the fundamentally first-order character of the unraveling and hence the simulation. It is the purpose of

*Present address: Abteilung für Quantenphysik, Universität Ulm, D-89069 Ulm, Germany.

this paper to show how this can be achieved.

In the following section we introduce an improved Monte Carlo method which provides a fourth-order simulation of the master equation (1) yet retains the simplicity of the method as described in [5] without the need to introduce waiting time distributions. We next examine the error measure in the Monte Carlo methods employed. This is followed by a section presenting the results of our investigation into the error of the Monte Carlo method and of the quantitative improvements from the fourth-order Monte Carlo method.

II. HIGHER-ORDER UNRAVELING

In this section we will present our proposal to arrive at higher accuracy results when using a modified Monte Carlo method and state the resulting changes from the standard method. The Monte Carlo or quantum jump method is based on the simulation of the conditioned evolution of either a density operator or a state vector [4]. At one point it is not, however, a rigorous implementation of the trajectory concept. Because this method discretizes time into small steps δt, a quantum jump [Eq. (4)] in the simulation takes a finite time δt, whereas in a simulation of quantum trajectories the information gained [5,15] from detection should instantaneously be used in conditioning the quantum state of the system. This pinpoints the subtle difference between conditioned trajectories and the slightly simpler idea of evaluating the probability of decay quanta at discrete time steps. The simplest way to remedy the fact that conditioning takes time in the simulation is to add evolution with the effective Hamiltonian to the projection step [Eq. (4)]. Having said this, the question arises at what point during the time interval δt we need to condition the quantum state according to the result of the detection process. First, it is worth noting that wherever we decide to do this, it would not change the accuracy of integrating the master equation in first order. Second, we may try to increase the accuracy by choosing a specific point in the interval δt. Let us integrate the master equation (1) to second order in δt :

$$\rho_S(t+\delta t) = \rho_S(t) + \frac{1}{2}\,\delta t\,([\mathcal{L}\rho_S]_t + [\mathcal{L}\rho_S]_{t+\delta t}) + O(\delta t^3)\,. \tag{6}$$

The terms that result from evaluating the right-hand side of this equation can be cast into the following form (see the Appendix):

$$\begin{aligned}\rho_S(t+\delta t) = {} & U\rho_S(t)U^\dagger + \frac{1}{2}\delta t UC\rho_S(t)C^\dagger U^\dagger \\ & + \frac{1}{2}\delta t CU\rho_S(t)U^\dagger C^\dagger \\ & + \frac{1}{2}\delta t^2 UCC\rho_S(t)C^\dagger C^\dagger U^\dagger + O(\delta t^3)\,. \end{aligned} \tag{7}$$

Here U denotes evolution under the influence of the effective Hamiltonian

$$U = \exp\left(-\frac{i}{\hbar}H_{\text{eff}}\,\delta t\right), \tag{8}$$

which we call the "no-jump" evolution. The four terms on the right-hand side of Eq. (7) represent four specific conditioned evolutions or *minitrajectories* that the system might follow. An expansion into minitrajectories is important because only then can the density matrix evolution (7) be simulated with pure states [as in Eqs. (3) and (4)]. The first minitrajectory in Eq. (7) represents evolution without any jump, the second and the third represent a jump followed by evolution without jumps and vice versa, respectively, and the fourth includes two successive jumps followed by no-jump evolution.

We see that it is not sufficient to specify one point in the interval δt at which to condition the density operator due to the quantum jump. We have to consider two points, at the beginning and at the end of δt, and also the possibility of two immediately successive quantum jumps in order to increase the accuracy in δt by one order.

We have pursued this idea to obtain results which are accurate up to fourth order (in δt). The master equation was integrated along the lines of a fourth-order Runge-Kutta method for ordinary differential equations. This was done using a MATHEMATICA package [16] of computer programs in order to ensure operator ordering was maintained. The resulting terms were ordered and cast into terms that represent minitrajectories. The result in fourth order then contains 13 minitrajectories (including the no-jump evolution) as follows:

$$\begin{aligned}\rho_S(t+\delta t) = {} & U_1\rho_S(t)U_1^\dagger + \tfrac{1}{8}\delta t U_1 C\rho_S(t)C^\dagger U_1^\dagger + \tfrac{1}{8}\delta t CU_1\rho_S(t)U_1^\dagger C^\dagger + \tfrac{3}{8}\delta t U_{\frac{1}{3}} CU_{\frac{2}{3}}\rho_S(t)U_{\frac{2}{3}}^\dagger C^\dagger U_{\frac{1}{3}}^\dagger \\ & + \tfrac{3}{8}\delta t U_{\frac{2}{3}} CU_{\frac{1}{3}}\rho_S(t)U_{\frac{1}{3}}^\dagger C^\dagger U_{\frac{2}{3}}^\dagger + \tfrac{1}{6}\delta t^2 U_{\frac{1}{2}} CU_{\frac{1}{2}} C\rho_S(t)C^\dagger U_{\frac{1}{2}}^\dagger C^\dagger U_{\frac{1}{2}}^\dagger + \tfrac{1}{6}\delta t^2 CU_{\frac{1}{2}} CU_{\frac{1}{2}}\rho_S(t)U_{\frac{1}{2}}^\dagger C^\dagger U_{\frac{1}{2}}^\dagger C^\dagger \\ & + \tfrac{1}{6}\delta t^2 U_{\frac{1}{2}} CCU_{\frac{1}{2}}\rho_S(t)U_{\frac{1}{2}}^\dagger C^\dagger C^\dagger U_{\frac{1}{2}}^\dagger + \tfrac{1}{24}\delta t^3 U_1 CCC\rho_S(t)C^\dagger C^\dagger C^\dagger U_1^\dagger + \tfrac{1}{24}\delta t^3 CU_1 CC\rho_S(t)C^\dagger C^\dagger U_1^\dagger C^\dagger \\ & + \tfrac{1}{24}\delta t^3 CCU_1 C\rho_S(t)C^\dagger U_1^\dagger C^\dagger C^\dagger + \tfrac{1}{24}\delta t^3 CCCU_1\rho_S(t)U_1^\dagger C^\dagger C^\dagger C^\dagger \\ & + \tfrac{1}{24}\delta t^4 U_1 CCCC\rho_S(t)C^\dagger C^\dagger C^\dagger C^\dagger U_1^\dagger + O(\delta t^5)\,. \end{aligned} \tag{9}$$

The subscripts on the non-Hermitian evolution U indicate the fraction of the time interval δt for which each particular U evolves the density operator, e.g., $U_{1/3} = \exp(-i H_{\text{eff}}\,\delta t/3\hbar)$. The way in which Eqs. (7) and (9) are turned into a Monte Carlo simulation is clear: each minitrajectory defines the conditioned evolution of the system and is assigned a specific probability with which it occurs, analogous to the jump and no-jump probabilities in the standard method. Just as in the standard procedure, a random number uniformly distributed between 0 and 1 is drawn to choose at random which of the minitrajectories will govern the system evolution in

the next time step δt. The no-jump evolution is tested first as this, for small δt, is the most likely minitrajectory. We note that the probability for evolution without detection remains unchanged as compared with the standard method and because the no-jump evolution is most likely the diversity of the minitrajectories hardly influences the necessary computing time. However, if the no-jump minitrajectory is not selected then one of the alternative trajectories in Eq. (9) must be chosen. For example, if the normalized state of the system at time t is $|\Psi(t)\rangle$ then the state of the system after evolution corresponding to the fourth minitrajectory in Eq. (9) is

$$|\Psi(t+\delta t)\rangle = \frac{1}{\mathcal{N}} e^{-i H_{\rm eff}\, \delta t/3\hbar}\, C\, e^{-i H_{\rm eff}\, 2\delta t/3\hbar}\, |\Psi(t)\rangle\,, \tag{10}$$

which includes a renormalization factor $\mathcal{N}$. The state $|\Psi\rangle$ is evolved with the effective Hamiltonian over two-thirds of the time step δt using a fourth-order Runge-Kutta integration step [5]. After projection with the Lindblad operator C the evolution is continued with the non-Hermitian Hamiltonian for the remaining third of the time step δt. Only then is the resulting state vector renormalized. The probability for this minitrajectory to occur is given by the product of the factor $3\delta t/8$ and the renormalization $\mathcal{N}$.

We note that the whole procedure described above [as in Eq. (9)] generalizes in a straightforward way to systems with more than one Lindblad operator C_k. As in the first-order unraveling procedure one simply extends Eq. (5) to include the additional decay channels through the $H_{\rm eff} = H_S - (i\hbar/2)\sum_k C_k^\dagger C_k$. However, in fourth order Eq. (9) must be generalized to a sum over all possible permutations of sequences of different jump operators C_k, e.g., the last term takes the form $(1/24)\,\delta t^4 \sum_{i,j,k,l} U_1 C_i C_j C_k C_l \rho_S(t) C_l^\dagger C_k^\dagger C_j^\dagger C_i^\dagger U_1^\dagger$.

The procedure we have described can be related to the unraveling of the master equation as it results from a formal integration of Eq. (1) [4], that is,

$$\begin{aligned}\rho(t) &= \exp\{\mathcal{L}(t-t_0)\}\,\rho(t_0) \\ &= \sum_{m=0}^{\infty} \int_{t_0}^{t} dt_m \int_{t_0}^{t_m} dt_{m-1} \cdots \int_{t_0}^{t_2} dt_1 \\ &\quad \times \{\, e^{(\mathcal{L}_0+\mathcal{L}_1)(t-t_m)} \mathcal{L}_2\, e^{(\mathcal{L}_0+\mathcal{L}_1)(t_m-t_{m-1})} \\ &\quad \times \mathcal{L}_2 \cdots \mathcal{L}_2\, e^{(\mathcal{L}_0+\mathcal{L}_1)(t_1-t_0)} \rho(t_0)\}\,. \end{aligned} \tag{11}$$

The rather complicated formula also applies for a small time step δt. The different terms in the sum contribute to different orders in δt. A first-order approximation to Eq. (11) replaces the sum over integrals by the sum terms $m = 0, 1$ and approximates the integral. The result is

$$\begin{aligned}\rho_S(t+\delta t) &= \sum_{m=0}^{\infty} \int_{t}^{t+\delta t} dt_m \int_{t}^{t_m} dt_{m-1} \cdots \int_{t}^{t_2} dt_1 \\ &\quad \times \{\, e^{(\mathcal{L}_0+\mathcal{L}_1)(t+\delta t-t_m)} \mathcal{L}_2\, e^{(\mathcal{L}_0+\mathcal{L}_1)(t_m-t_{m-1})} \mathcal{L}_2 \cdots \mathcal{L}_2\, e^{(\mathcal{L}_0+\mathcal{L}_1)(t_1-t)} \rho(t)\} \\ &= e^{(\mathcal{L}_0+\mathcal{L}_1)\,\delta t} \rho_S(t) \;+\; \delta t\, e^{(\mathcal{L}_0+\mathcal{L}_1)\,\delta t} \mathcal{L}_2 \rho_S(t) \;+\; O(\delta t^2)\,. \end{aligned} \tag{12}$$

This result leads to a procedure as described by Eqs. (3) and (4), the only difference being the evolution with the non-Hermitian Hamiltonian that follows the projection [Eq. (4)]. Higher than second order approximations to Eq. (11) involve approximations to multiple integrals to higher than first order. Using the trapezian rule extended to multiple integrals we arrive at Eq. (9) as an approximation to Eq. (11). It is worth noting that Eq. (9) is not unique in the sense that it integrates the master equation (1) to fourth order.

III. ERROR MEASURE

Next we will give a description of how to assign an error measure to Monte Carlo results. Typical results from the Monte Carlo method are time evolutions of observables calculated as an average of (say) N single trajectories. These N trajectories constitute a sample drawn at random from the universe of trajectories. The outcome of an observable (say) x at time step j in the time evolution is

$$\bar{x}|_j = \frac{1}{N} \sum_{i=1}^{N} x_i|_j\,, \tag{13}$$

an average over the outcomes $x_i|_j$ from single trajectories i at time step j. The number we choose as an error measure for a particular result is calculated as

$$\beta^2 = \frac{1}{n} \sum_{j=1}^{n} (\bar{x}|_j - x_0|_j)^2 = \frac{1}{n} \sum_{j=1}^{n} \beta_j^2\,, \tag{14}$$

where $x_0|_j$ is the exact result that may be obtained from an analytical solution and the sum over j means averaging the square of the number β_j over the n time steps in the evolution. By examination of one of these sum terms ${\beta_j}^2$ we find

$$\beta_j^2 = \frac{1}{N} \sum_{i=1}^{N} (x_i|_j - x_0|_j)^2 - (s_x|_j)^2\,, \tag{15}$$

where $(s_x|_j)^2$ is the squared standard deviation of the sample

$$(s_x|_j)^2 = \frac{1}{N} \sum_{i=1}^{N} (x_i|_j - \bar{x}|_j)^2\,. \tag{16}$$

From the principles of the Monte Carlo method we know

that taking into account the whole universe of trajectories the mean yields the analytical result $x_0|_j$. Although we do not (and cannot) take into account all trajectories in the universe, we might take the sum in Eq. (15) to approximate the squared standard deviation in the universe $(\sigma_x|_j)^2$:

$$(\sigma_x|_j)^2 = \frac{1}{N}\sum_{i=1}^{N}(x_i|_j - x_0|_j)^2 . \tag{17}$$

Furthermore, for the case of a normal distribution we can use

$$\sigma_x = s_x\sqrt{\frac{N}{N-1}}, \tag{18}$$

so that

$$\beta_j = \frac{\sigma_x|_j}{\sqrt{N}} \tag{19}$$

is the standard error of the average. Hence the number β we chose as an error measure is a root mean squared average of the standard error along the time evolution and in particular we expect it to be proportional to $1/\sqrt{N}$.

IV. RESULTS

We have investigated the improvement gained from implementing the higher-order unraveling formula [Eq. (9)] by looking at the problem of resonance fluorescence from a two-level system [11]. In a rotating frame the effective Hamiltonian is

$$H_{\text{eff}} = \hbar\Delta\,\sigma^+\sigma^- + \hbar(g\sigma^+ + g^*\sigma^-) - \frac{i\hbar}{2}\gamma\,\sigma^+\sigma^-, \tag{20}$$

where σ^+, σ^- are operators for the two-level system which flip the state of excitation, $\Delta = \omega - \Omega$, denotes detuning between the two-level transition frequency ω and the field mode frequency Ω, and $g = -\frac{1}{2}\wp\mathcal{E}_\Omega$ incorporates the strength $\mathcal{E}_\Omega$ of the driving field and the dipole matrix element $\wp$. The decay constant γ describes the coupling to the vacuum and the Lindblad operator C in Eq. (2) becomes $\sqrt{\gamma}\sigma^-$. For our simulations we chose $g/\gamma = 1$ and zero detuning. In Fig. 1 we show two Monte Carlo method results, one using the first-order unraveling as given by Eqs. (2) and (3) (dashed line), the other one using the fourth-order unraveling formula [Eq. (9)] (dotted line). Note that in implementing Eq. (9) the last six terms are not needed in this problem because $(\sigma^-)^2 = (\sigma^+)^2 = 0$. The fourth-order result is hard to distinguish from the analytical solution (solid line) obtained by solving the master equation. It can clearly be seen that for this sample size N and time step δt, the fourth-order Monte Carlo method converges accurately. The first-order method would have required a much smaller time step to achieve the same accuracy. The two parameters N and δt compete in their influence on the error. Having chosen a particular step size δt, an increase in N will not always continue to improve the error. At some point, the first-order character of the decision between no-jump and jump at every time step [Eqs. (3) and (4)] will start to dominate, so that increasing the sample size does not reduce the error any further. This leveling out is the most prominent feature of Fig. 2. As we expected from the discussion above, the error measure first shows a $1/\sqrt{N}$ dependence before it begins

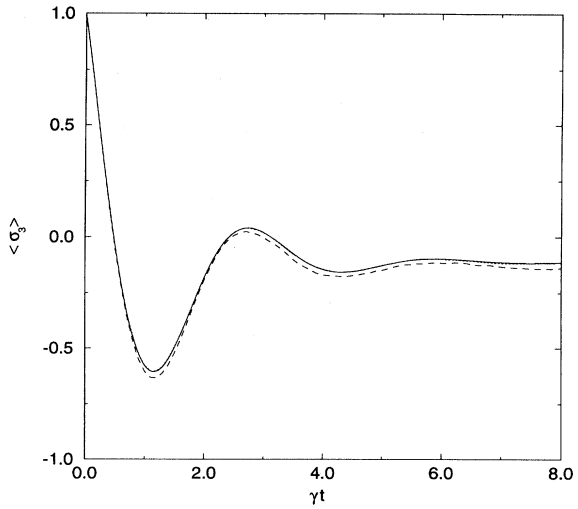

FIG. 1. Ensemble averaged time evolution for the expectation value $\langle\sigma_3\rangle$ (inversion in the two-level system). The dotted line shows a sample of 250 000 trajectories obtained by the fourth-order Monte Carlo method ($g/\gamma = 1$, $\gamma\delta t = 0.1$, and zero detuning). It is hard to distinguish the dotted line from the solid line showing the analytical result. The dashed line shows a sample of 250 000 trajectories obtained by the first-order Monte Carlo method for the same parameters.

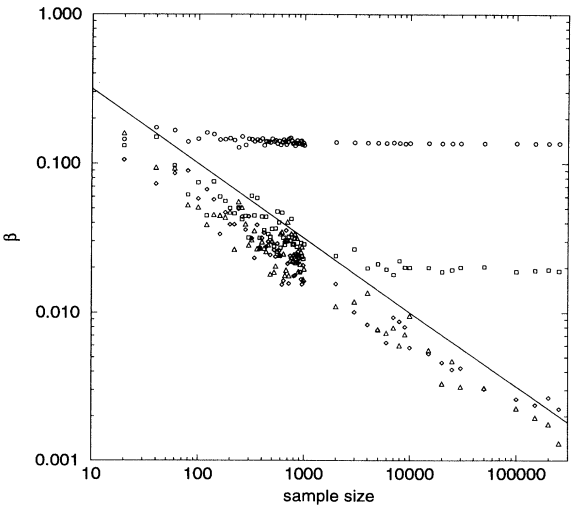

FIG. 2. The error measure β as an average over the time evolution from $\gamma t = 0$ to $\gamma t = 8$ for different sample sizes and time steps using the first-order method. Sample sizes range from 20 to 250 000. The time steps are $\gamma\delta t = 1, 0.1, 0.01$, and 0.001 and are depicted by the symbols ○, □, ◇, and △, respectively. Other parameters are the same as in Fig. 1. The solid line shows $1/\sqrt{N}$.

to flatten out and remain constant with increasing N, owing to the constant influence of the step size δt. The remaining errors at very large N roughly depend linearly on the size of δt. This means that we can estimate the required sample size and time step to achieve a particular accuracy.

We now reexamine the same evolution, but using the fourth-order unraveling formula [Eq. (9)]. The result is shown in Fig. 3. Only for the largest time step δt was the region of constant error reached within the sample sizes we chose. By comparison with the first-order method, the accuracy achieved with a given time step is much greater so that we can drastically increase the size of the time step and still obtain results of the same accuracy. Using the first-order method, we need to reduce the time step to $\delta t = 10^{-3}$ in order to achieve an error of the order of 10^{-3}. The fourth-order method allows us to use $\delta t = 10^{-1}$, which is two orders of magnitude larger. We note that the higher complexity of Eq. (9), as compared to Eqs. (3) and (4), leads to only a slight increase in computing time. So with a mean of four jumps occurring during a time evolution that consists of 8000 steps, this improvement means that if the fourth-order method is required to perform at the same accuracy as a first-order unraveling, much larger time steps can be used and there can be a considerable saving in computational effort (by orders of magnitude).

We have also applied the fourth-order unraveling formula [Eq. (9)] to a more complex system: the problem of the Jaynes-Cummings revivals with cavity loss. Making use of a large step size δt, we can show that also for this system the Monte Carlo method converges accurately. Especially when insisting on high accuracy results this is an enterprise that would have taken significantly longer given modest personal computer or workstation computing power and using the first-order method.

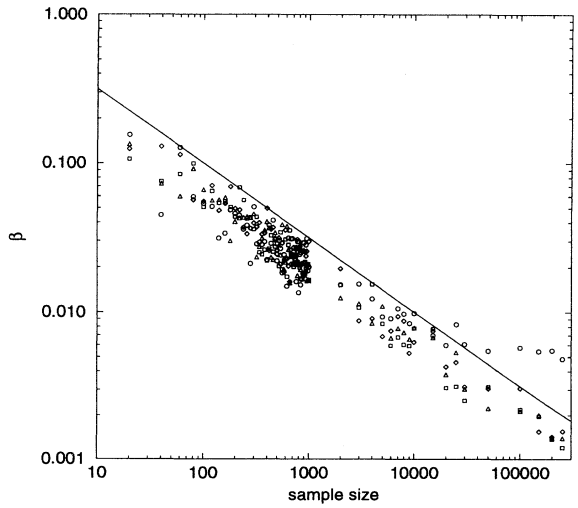

FIG. 3. The error measure β as an average over the time evolution from $\gamma t = 0$ to $\gamma t = 8$ for different sample sizes and time steps using the fourth-order method. Sample sizes range from 20 to 250 000. The time steps are $\gamma \delta t = 1, 0.1, 0.01$, and 0.001 and are depicted by the symbols ○, □, ◇, and △, respectively. Other parameters are the same as in Fig. 1. The solid line shows $1/\sqrt{N}$.

V. CONCLUSIONS

We have presented a fourth-order Monte Carlo method to simulate dissipative evolution of quantum systems. Using an error measure which is a squared mean of the standard error of the average from the single trajectories, we have shown the competing influence of sample size N and size of the time step δt on the error in Monte Carlo results. In the region of sample sizes where the error from the finite size of the sample dominates, we find a $1/\sqrt{N}$ dependency of the error, whereas in the region where the finite time step dominates the error, it remains a constant with increasing size of the sample. The linear error dependence on time step size δt for very large samples enables us to estimate an error given a particular time step and sample size in our model problem. We have shown how the modified fourth-order Monte Carlo method can reduce this error by two orders of magnitude while increasing computing time only marginally. Alternatively, the same accuracy can be achieved by the present method in a computing time that is two orders of magnitude shorter. It is not necessary to calculate waiting time distributions and the implementation on a computer remains as simple as for the standard method. Moreover, the method can be directly applied without the need of prior analytical calculation.

ACKNOWLEDGMENTS

This work was supported in part by the United Kingdom Engineering and Physical Sciences Research Council, the European Community, and the German Academic Exchange Service.

APPENDIX: THE SECOND-ORDER UNRAVELING

In this appendix we will show some of the details of the second order unraveling, that is, we give the steps needed to go from Eq. (6) to Eq. (7). We start by performing a Taylor expansion on Eq. (6) to obtain

$$\rho_S(t+\delta t) \simeq \left(1 + \delta t \mathcal{L} + \frac{\delta t^2}{2}\mathcal{L}^2\right)\rho_S(t) \qquad \text{(A1)}$$

in second order. We work to second order in δt throughout this appendix and for convenience we set $\hbar = 1$ in this appendix only. The Liouville operator $\mathcal{L}$ is given in Eq. (2) and may be used to obtain

$$\mathcal{L}^2\rho_S(t) \simeq -H_S^2\rho_S(t) + 2H_S\rho_S(t)H_S + \frac{i}{2}H_SC^\dagger C\rho_S(t) + iH_S\rho_S(t)C^\dagger C - iH_SC\rho_S(t)C^\dagger - \rho_S(t)H_S^2 - iC^\dagger C\rho_S(t)H_S$$
$$-\frac{i}{2}\rho_S(t)C^\dagger CH_S + iC\rho_S(t)C^\dagger H_S + \frac{i}{2}C^\dagger CH_S\rho_S(t) + \frac{1}{4}C^\dagger CC^\dagger C\rho_S(t)$$
$$+\frac{1}{2}C^\dagger C\rho_S(t)C^\dagger C - \frac{1}{2}C^\dagger CC\rho_S(t)C^\dagger - \frac{i}{2}\rho_S(t)H_SC^\dagger C + \frac{1}{4}\rho_S(t)C^\dagger CC^\dagger C - \frac{1}{2}C\rho_S(t)C^\dagger C^\dagger C$$
$$-iCH_S\rho_S(t)C^\dagger + iC\rho_S(t)H_SC^\dagger - \frac{1}{2}CC^\dagger C\rho_S(t)C^\dagger - \frac{1}{2}C\rho_S(t)C^\dagger CC^\dagger + CC\rho_S(t)C^\dagger C^\dagger. \tag{A2}$$

Now, as in the first-order unraveling, we anticipate a term in the expansion to be of the form $U\rho_S(t)U^\dagger$, where U is given in Eq. (8). The factor $U\rho_S(t)U^\dagger$ is simply the density matrix version of Eq. (3). To evaluate $U\rho_S(t)U^\dagger$ we first need the second-order expansion of U which is

$$U \simeq 1 + \delta t\left(-iH_S - \frac{1}{2}C^\dagger C\right) + \frac{\delta t^2}{2}\left(-H_S^2 + \frac{1}{4}C^\dagger CC^\dagger C + \frac{i}{2}H_SC^\dagger C + \frac{i}{2}C^\dagger CH_S\right). \tag{A3}$$

This then leads us to the second-order expansion of $U\rho_S(t)U^\dagger$,

$$U\rho_S(t)U^\dagger \simeq \rho_S(t) + \delta t\left(-iH_S\rho_S(t) - \frac{1}{2}C^\dagger C\rho_S(t) + i\rho_S(t)H_S - \frac{1}{2}\rho_S(t)C^\dagger C\right)$$
$$+\frac{\delta t^2}{2}\left(2H_S\rho_S(t)H_S + \frac{1}{2}C^\dagger C\rho_S(t)C^\dagger C + iH_S\rho_S(t)C^\dagger C - iC^\dagger C\rho_S(t)H_S - H_S^2\rho_S(t) + \frac{1}{4}C^\dagger CC^\dagger C\rho_S(t)\right.$$
$$\left.+\frac{i}{2}H_SC^\dagger C\rho_S(t) + \frac{i}{2}C^\dagger CH_S\rho_S(t) - \rho_S(t)H_S^2 + \rho_S(t)C^\dagger CC^\dagger C - \frac{i}{2}\rho_S(t)C^\dagger CH_S - \frac{i}{2}\rho_S(t)H_SC^\dagger C\right). \tag{A4}$$

Now if we subtract this expression for $U\rho_S(t)U^\dagger$ from the second-order expansion for $\rho_S(t+\delta t)$, which is Eq. (A1) with $\mathcal{L}^2\rho_S(t)$ from Eq. (A2), we obtain the residue

$$\rho_S(t+\delta t) - U\rho_S(t)U^\dagger \simeq \delta tC\rho_S(t)C^\dagger + \frac{\delta t^2}{2}\left(-iH_SC\rho_S(t)C^\dagger + iC\rho_S(t)C^\dagger H_S - \frac{1}{2}C^\dagger CC\rho_S(t)C^\dagger - \frac{1}{2}C\rho_S(t)C^\dagger C^\dagger C\right.$$
$$-iCH_S\rho_S(t)C^\dagger$$
$$\left.+iC\rho_S(t)H_SC^\dagger - \frac{1}{2}CC^\dagger C\rho_S(t)C^\dagger - \frac{1}{2}C\rho_S(t)C^\dagger CC^\dagger + CC\rho_S(t)C^\dagger C^\dagger\right). \tag{A5}$$

These terms are to be assigned to minitrajectories. The first term $C\rho_S(t)C^\dagger$ is in the correct form for a minitrajectory and corresponds to the first-order Eq. (4) when placed in a density matrix form. The last term $CC\rho_S(t)C^\dagger C^\dagger$ is also in the correct form, but the remaining terms are not obviously minitrajectories (i.e., they are not Hermitian, etc.). However, we note that, to first order in δt, we can expand a new minitrajectory $UC\rho_S(t)C^\dagger U^\dagger$ as

$$UC\rho_S(t)C^\dagger U^\dagger \simeq C\rho_S(t)C^\dagger + \delta t\left(-iH_SC\rho_S(t)C^\dagger - \frac{1}{2}C^\dagger CC\rho_S(t)C^\dagger + iC\rho_S(t)C^\dagger H_S - \frac{1}{2}C\rho_S(t)C^\dagger C^\dagger C\right). \tag{A6}$$

If we multiply this equation by $\delta t/2$ we see that it results in half of the first term on the right-hand side of Eq. (A5) and exactly the second through to the fifth terms of Eq. (A5). We conclude that we need only $\delta tUC\rho_S(t)C^\dagger U^\dagger/2$ to obtain almost half of Eq. (A5). The sixth to ninth terms of Eq. (A5) are easily found to be the minitrajectory $\delta tCU\rho_S(t)U^\dagger C^\dagger/2$. As mentioned, the last term is already a minitrajectory, although to second order in δt we have

$$CC\rho_S(t)C^\dagger C^\dagger \simeq UCC\rho_S(t)C^\dagger C^\dagger U^\dagger \tag{A7}$$

and we may use either form. In Eq. (7) we have used the second form because it is closer to the terms appearing in higher orders such as the fourth order unraveling in Eq. (9). This completes the proof of Eq. (7).

[1] W.H. Louisell, *Quantum Statistical Properties of Radiation* (Wiley, New York, 1973).
[2] G. Lindblad, Commun. Math. Phys. **48**, 119 (1976).
[3] C.W. Gardiner, A.S. Parkins, and P. Zoller, Phys. Rev. A **46**, 4363 (1992).
[4] H.J. Carmichael, *An Open Systems Approach to Quantum Optics*, Lecture Notes in Physics m18 (Springer-Verlag, Berlin, 1993).
[5] J. Dalibard, Y. Castin, and K. Mølmer, Phys. Rev. Lett. **68**, 580 (1992); K. Mølmer, Y. Castin, and J. Dalibard, J. Opt. Soc. Am. B **10**, 524 (1993).
[6] Y. Castin, J. Dalibard, and K. Mølmer, in *Atomic Physics 13,* edited by H. Walther, T.W. Hänsch, and B. Neizert (AIP, New York, 1993), p. 143.
[7] H.M. Wiseman and G.J. Milburn, Phys. Rev. A **47**, 1652 (1993).
[8] H.J. Carmichael, S. Singh, R. Vyas, and P.R. Rice, Phys. Rev. A **39**, 1200 (1989).
[9] L. Tian and H.J. Carmichael, Phys. Rev. A **46**, 6801 (1992).
[10] C. Cohen-Tannoudji, B. Zambon, and E. Arimondo, J. Opt. Soc. Am. B **10**, 2107 (1993).
[11] R. Dum, A.S. Parkins, P. Zoller, and C.W. Gardiner, Phys. Rev. A **46**, 4382 (1992).
[12] B.M. Garraway and P.L. Knight, Phys. Rev. A **49**, 1266 (1994).
[13] B.M. Garraway and P.L. Knight, Phys. Rev. A **50**, 2548 (1994).
[14] B.M. Garraway, P.L. Knight, and J. Steinbach, Appl. Phys. B (to be published).
[15] D.T. Pegg and P.L. Knight, Phys. Rev. A **37**, 4303 (1988).
[16] MATHEMATICA package 0202-273, A. Hsieh and E. Yehudai, a package for symbolic high-energy physics calculations, 1991.